FACETS
a multidisciplinary open access science journal

RESEARCH ARTICLE

The reproducibility of remotely piloted aircraft systems to monitor seasonal variation in submerged seagrass and estuarine habitats

T.S. Prystay[a]*, G. Adams[a], B. Favaro[b], R.S. Gregory[c], and A. Le Bris[a]

[a]Centre for Fisheries Ecosystems Research, Fisheries and Marine Institute, Memorial University of Newfoundland, St. John's, NL A1C 5R3, Canada; [b]Faculty of Science and Horticulture, Kwantlen Polytechnic University, Surrey, BC V3W 2M8, Canada; [c]Fisheries and Oceans Canada, Ecological Sciences Section, Northwest Atlantic Fisheries Centre, St. John's, NL A1C 5X1, Canada

*tanya.prystay@mi.mun.ca

Citation: Prystay TS, Adams G, Favaro B, Gregory RS, and Le Bris A. 2023. The reproducibility of remotely piloted aircraft systems to monitor seasonal variation in submerged seagrass and estuarine habitats. FACETS 8: 1–22. doi:10.1139/facets-2022-0149

Handling Editor: Maud Ferrari

Received: June 26, 2022

Accepted: November 3, 2022

Published: March 2, 2023

Published by: Canadian Science Publishing

Abstract

Seasonal variation in seagrass growth and senescence affects the provision of ecosystem services and restoration efforts, requiring seasonal monitoring. Remotely piloted aircraft systems (RPAS) enable frequent high-resolution surveys at full-meadow scales. However, the reproducibility of RPAS surveys is challenged by varying environmental conditions, which are common in temperate estuarine systems. We surveyed three eelgrass (*Zostera marina*) meadows in Newfoundland, Canada, using an RPAS equipped with a three-color band (red, green, blue [RGB]) camera, to evaluate the seasonal reproducibility of RPAS surveys and assess the effects of flight altitude (30–115 m) on classification accuracy. Habitat percent cover was estimated using supervised image classification and compared to corresponding estimates from snorkel quadrat surveys. Our results revealed inconsistent misclassification due to environmental variability and low spectral separability between habitats. This rendered differentiating between model misclassification versus actual changes in seagrass cover infeasible. Conflicting estimates in seagrass and macroalgae percent cover compared to snorkel estimates could not be corrected by decreasing the RPAS altitude. Instead, higher altitude surveys may be worth the trade-off of lower image resolution to avoid environmental conditions shifting mid-survey. We conclude that RPAS surveys using RGB imagery alone may be insufficient to discriminate seasonal changes in estuarine subtidal vegetated habitats.

Key words: drone, eelgrass, remotely piloted aircraft systems, quadrats, altitude, survey reproducibility, temperate

Introduction

Seagrasses occur along the coastlines of every continent except for Antarctica (Short et al. 2001) and support numerous ecosystem functions and services including food provision, water purification, fish habitat, and carbon sequestration (Nordlund et al. 2016). Global declines of seagrass meadows and resulting loss of ecosystem functions and services are major concerns in conservation ecology (Barbier et al. 2011; Orth et al. 2006; Salinas et al. 2020; Waycott et al. 2009; Worm et al. 2006). Increasing efforts have been made globally to monitor and restore seagrass meadows (Orth et al. 2020; Tan et al. 2020) and to quantify the services they provide (Nordlund et al. 2018, 2016).

Strong seasonality in light availability and other environmental conditions (e.g., freshwater influx, temperature) in cold-temperate estuarine regions results in marked periods of growth and senescence in seagrass (Hemminga and Duarte 2000). Such seasonal variation can affect the provision of ecosystem functions and services (Sonoki et al. 2016) and the success of restoration efforts (Li et al. 2014; Zimmerman et al. 1995). This supports the need for seasonal monitoring of seagrass meadows (Björk et al. 2008; Kirkman 1996), which may further be used to determine the optimal season for restoration actions (Li et al. 2014; Zimmerman et al. 1995) and for annual monitoring.

Seasonal monitoring of seagrass and adjacent estuarine benthic habitats improves understanding of changes in the meadow and the provision of ecosystem services but requires methods that can detect fine-scale seasonal variability in cover and extent of the different benthic habitats (Chand and Bollard 2022), while surveying at the meadow-scale (often several hectares). These methods must also be reproducible, meaning they produce similar quality data across surveys. Numerous approaches have been used for seasonal monitoring of seagrass meadows including wading/snorkel/SCUBA surveys (Cho et al. 2017; Fourqurean et al. 2001; Short et al. 2006), aerial photos (Reise and Kohlus 2008), satellite imagery (Lyons et al. 2013), and acoustic surveys (Sonoki et al. 2016). Remote sensing applications for seagrass monitoring are generally used to measure seagrass extent (Lyons et al. 2013), whereas wading/snorkel/SCUBA approaches reveal smaller scale and higher resolution details such as shifts in percent cover of seagrass, shoot density, and species composition (i.e., presence of macroalgae; Fourqurean et al. 2001; Short et al. 2006). More recently, remotely piloted aircraft systems (RPAS; i.e., drones) have been applied to monitor seasonal variation in seagrass extent and structure (Chand and Bollard 2022; Krause et al. 2021) due to their ability to collect high resolution images frequently and at a relatively low cost and their potential to automate part of the work (Colefax et al. 2018; Joyce et al. 2018). By reducing monitoring costs, RPAS present a promising approach for seagrass monitoring because seagrass monitoring is widespread and conducted by groups that are resource and time limited, including academics, non-profit, and government entities seeking to optimize monitoring resources. However, studies on seasonal reproducibility of RPAS did not include delineation of other adjacent estuarine habitats (e.g., other species of submerged aquatic vegetation), which can be challenging to spectrally separate (Duffy et al. 2018; Tait et al. 2019), and focused RPAS surveys on limited portions of a meadow. Examining whether full-meadow scale seasonal RPAS surveys can reliably detect changes in seagrass extent, percent cover, and differentiate seagrass from other habitats would determine whether RPAS effectively bridge the gap between remote sensing and wading/snorkel/SCUBA surveys.

To detect seasonal changes in seagrass, RPAS surveys must be reproducible. However, a major challenge with RPAS surveys is that image quality quickly diminishes in less than optimal environmental conditions (e.g., cloud cover, wind, turbidity, high-tide), challenging seagrass identification (Joyce et al. 2018; Nahirnick et al. 2019a, 2019b). These environmental changes can shift within minutes/hours and mid-survey (e.g., tide, cloud cover, sun angle) as well as over longer time periods, including seasonally and annually. Additionally, seagrass blades may fold over at low tide or when there is a fast current, increasing the likelihood of overestimating seagrass density. While recent studies have provided roadmaps of ideal environmental conditions for RPAS surveys of seagrass (e.g., Joyce et al. 2018; Nahirnick et al. 2019b; Tait et al. 2019; Yang et al. 2020), studies evaluating the efficacy of surveys have generally focused on one-time occurrences in tropical regions (e.g., Ellis et al. 2020) or portions of a meadow (Barrell and Grant 2015; Duffy et al. 2018; Ellis et al. 2020; Konar and Iken 2018; Krause et al. 2021). In temperate regions, high environmental variability, including rapid shifts in cloud cover, wind, and chemistry of estuarine waters (e.g., tannins), challenges RPAS surveys (Nahirnick et al. 2019a, 2019b). The source and frequency of environmental variability in temperate estuarine systems often differ among seasons, making seasonal monitoring even more challenging as it can be difficult to collect comparable images. For instance, seasonal

effects include higher rainfall in the fall and snowmelt in the spring, whereas daily variation includes changing water levels due to tide and rainfall and varying tannin concentrations depending on riverine discharge. Therefore, an evaluation of survey accuracy and reproducibility in such systems is necessary if RPAS are to be used to monitor changes in habitat extent, percent cover, and adjacent benthic habitat over time.

Detecting fine-scale seasonal changes in seagrass meadows requires collecting high spatial resolution surveys. RPAS image resolution is inversely proportional to altitude, and fewer details in images collected at higher altitudes can complicate habitat classification and survey reproducibility (Seifert et al. 2019). However, increasing survey altitude reduces flight time as larger areas are covered per image, which limits the risk of environmental conditions such as sun angle and tide, which change within minutes/hours, from changing mid-survey (Joyce et al. 2018) and enables more frequent surveys. Furthermore, varying flight altitude may affect the reproducibility of RPAS surveys in multiple ways. Ellis et al. (2020) showed the effect of altitude on image classification depended on habitat when surveying at increasing altitude, presumably due to different levels of spectral separability among habitats. Sand cover estimates increased with altitude, whereas seagrass estimates decreased, and mangrove, coral, and open water estimates were unaffected. These differences highlight the need to better understand the trade-offs associated with altitude, including how they relate to the structure of the meadow (e.g., fragmented vs. continuous) and location in the meadow (i.e., edge vs. middle) to conduct reproducible seasonal surveys of seagrass meadows.

The first objective of this study was to test the reproducibility for RPAS to monitor seasonal changes in eelgrass (*Zostera marina*) meadows and adjacent benthic estuarine habitats in cold-temperate ecosystems. This represents the first study to evaluate the capacity of RPAS surveys to detect seasonal (i.e., summer vs. fall) variation in meadow extent, percent cover, and macroalgae cover across multiple sites of relatively large area (~50 ha). We compared orthomosaics and image classification accuracies across surveys to assess the reproducibility of RPAS for estimating seasonal changes in seagrass extent in three sites. RPAS estimates of habitat percent cover and species composition were compared to complementary snorkel quadrat surveys to evaluate whether both methods yielded similar seasonal trends in eelgrass and macroalgae percent cover. Finally, since flight altitude implies trade-offs between image resolution and survey time, our second objective was to evaluate the effects of flying at a high altitude (e.g., 30 m vs. 115 m) on estimates of seasonal changes in percent cover.

Methods

Study sites

We surveyed three sites with eelgrass meadows in Placentia Bay, Newfoundland: North Harbour, Swift Current, and Baie de l'Eau (**Fig. 1**). North Harbour and Baie de l'Eau are shallow meadows, growing to a maximum depth of <1 m (below chart datum). The eelgrass meadow in North Harbour is divided into two main patches, whereas the Baie de l'Eau meadow is fragmented throughout. The Swift Current meadow is continuous, where eelgrass maximum depth reaches 0–2 m (below chart datum) depending on the section of the meadow. Macroalgae, predominantly *Fucus spp.*, *Chorda filum, Ascophyllum nodosum,* and *Chondrus crispus*, also occur in each meadow.

RPAS surveys

We conducted two surveys per site in 2020: one in the summer (July 6–22) and one in the fall (September 21–October 13) (**Table 1**). Markers for ground control points (GCPs) and check points (CPs) were placed onshore surrounding the eelgrass meadows (see *RPAS data processing* for application; see Supporting Information for methods of deploying GCPs and CPs).

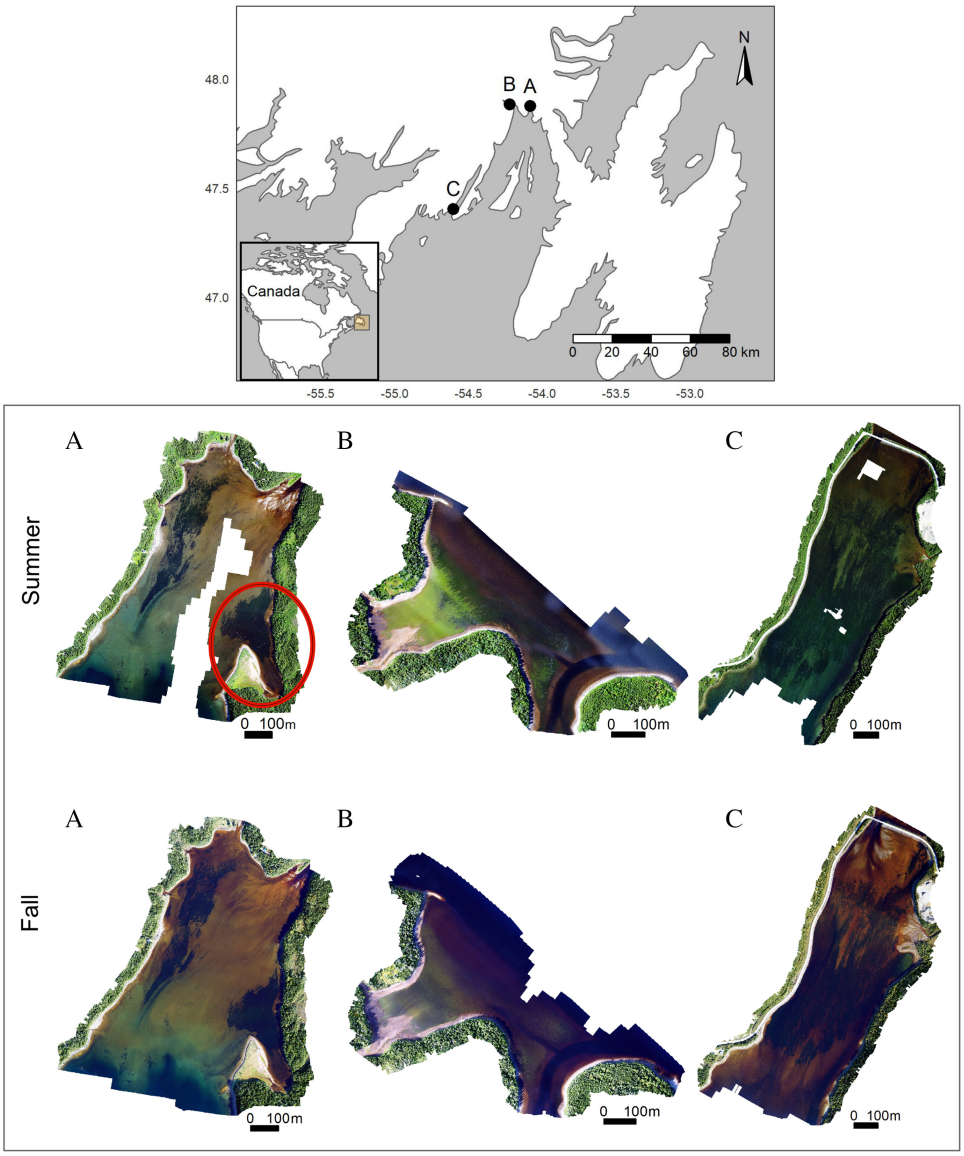

Fig. 1. Map of survey locations (top) and seasonal orthomosaics of (A) North Harbour, (B) Swift Current, and (C) Baie de l'Eau, created using a remotely piloted aircraft system (RPAS) flown at 115 m altitude. Images were collected in the summer and fall of 2020. Red circle in (A) outlines subsite Caplin Cove. Map of survey location (top) was created using shapefiles from the R package tmap (Tennekes 2018) and from Natural Earth (2021) and using the WGS84 coordinate reference system.

RPAS surveys were conducted using a DJI Matrice 210 RTK equipped with a 24 mm lens Zenmuse X7 camera and a polarized lens. Flight plans were executed using the DJI Pilot application. Camera settings, namely white balance, shutter speed, and ISO, were set prior to each survey while the RPAS hovered at 115 m altitude (same as the survey altitude; **Table S1**). We conducted the surveys when there was no cloud cover (0%) and in low wind conditions (i.e., ≤10 km/h) according to the European Centre for Medium-Range Weather Forecasts model (windy.com), while also avoiding days following a rain event when turbidity would be elevated. Such weather combinations are uncommon

Table 1. Summary of snorkel survey and remotely piloted aircraft system (RPAS) survey, including the RPAS survey duration, number of ground control points (GCPs), and control points (CPs) used to create the orthoimage, survey coverage, flight altitude, flight speed, and tidal height.

Site	Season	Sample date and time (day/month/year h:m)	GCPs/CPs	Survey area (ha)	Flight altitude (m)	Flight speed (ms^{-1})	Tide height (m)	Eelgrass area (ha)
Swift Current	Summer	06/07/2020 16:45–17:25	4/2	30.9	115	6	0.7	5.23
	Fall	21/09/2020 15:43–16:42	5/2				0.9	7.38
North Harbour	Summer	18/07/2020 9:19–10:17	5/3	52.3	115	6	1.7	5.76
	Fall	06/10/2020 9:29–10:42	5/3				1.5	5.46
Baie de l'Eau	Summer	22/07/2020 9:19–10:17	6/3	70.1	115	6	2.3	14.54
	Fall	13/10/2020 9:54–11:42	6/3				0.9	9.04
Capelin Cove	Summer	18/07/2020 10:30–10:40		2.7	25	1.3	1.3	
Capelin Cove	Summer	18/07/2020 10:43–10:52		4.4	50	2.6	1.3	
Capelin Cove	Summer	18/07/2020 10:22–10:27		3.2	100	5.2	1.3	

Note: The number of GCPs/CPs and their placement were limited by tree cover and substrate that was stable yet penetrable by the rebar (see Supporting Information for GCPs and CPs deployment). Total estimated eelgrass area (m) was calculated by classifying the RPAS imagery using supervised image classification with random forest analysis.

in Newfoundland; therefore, we could not control for tidal height among surveys (Table 1). Instead, we prioritized consistent reflectance across our survey, which is necessary to apply automated classification during post-processing. We also conducted the surveys during early morning or late afternoon (Table 1), when the sun was between 20 and 40° to minimize glare (Ellis et al. 2020; Mount 2005; Nahirnick et al. 2019b) and to avoid wave-induced disturbances. Only Swift Current was surveyed in the afternoon because it has a short fetch. For each site survey, the RPAS was programmed to fly at 115 m altitude while moving 6 ms^{-1} and to capture photos continuously with the camera nadir facing (i.e., lens pointing directly below the camera). Images were collected with 80% front overlap and 70% side overlap.

Collecting field ground-truth data

We collected GoPro images to create training and validation data for the RPAS supervised image classification. This involved collecting images of the seafloor throughout the site using a GoPro camera and georeferencing these images using a handheld GPS (Garmin *e*trex 20×^{TM}). The images were analyzed to identify the dominant habitat (eelgrass, macroalgae, unvegetated) and then used to train and validate the image classification model of the RPAS survey (see *RPAS data processing*). Training and validation data were collected for each site within a week of the RPAS survey.

We then collected snorkel quadrat survey data to evaluate the reproducibility of the RPAS survey to measure eelgrass and macroalgae percent cover. For the snorkel transect survey, we marked six transects in each site using rebar embedded into the shore and georeferenced using a GPS. Transect locations were chosen such that two intersected the middle, two intersected the edge, and two were

outside of the meadows (Fig. S1). Snorkel transects followed a 50 m lead line marked at 10 m intervals starting 20 m from the water's edge to mark the quadrat placement (Fig. S1). Using a 1 m^2 quadrat divided into a 10 cm × 10 cm grid, eelgrass and macroalgae densities were estimated as the percentage of grid cells within the quadrat with shoots ($n_{quadrat/site} = 24$). If a grid cell had both eelgrass and macroalgae, it was counted as both. If no eelgrass or macroalgae was present, the grid cell was classified as unvegetated. Similar to the RPAS surveys, we conducted two snorkel quadrat surveys for each site, once in the summer and again in the fall. All snorkel quadrat surveys were performed by the same snorkeller and within a month of the RPAS survey.

RPAS data processing

Orthomosaics were generated using Agisoft Photoscan (v.1.4.5). We divided the GCP/CP markers to use 70%–80% of the markers to optimize the position accuracy of the orthomosaic, and the remainder to evaluate error in the orthomosaic (Table 1). Orthomosaics were exported at a 10 cm × 10 cm pixel resolution to match the size of the grid cells in the quadrat used during the snorkel survey (see *Collecting field ground-truth data*), which also reduces the pixel variability in our orthomosaics.

Orthomosaics were analyzed separately using random forest supervised image classification via the "superClass" function in the RStoolbox (v. 0.2.6.; Leutner et al. 2019) package in RStudio (v. 1.2.5033). We defined the training data according to the red, green, and blue (RGB) color composites for the pixel associated with each training point (Fig. 2). This was done by projecting the coordinates of the GoPro imagery onto the orthomosaic in ArcMap (v. 10.7). Given that the GPS we used to georeference the training data has an accuracy of 3.65 m, we inspected the 100 ± 20 training points collected for each RPAS survey to ensure that the habitat attributed to the point matched the location of the point (e.g., eelgrass was not in the middle of unvegetated habitat). If a point was obviously wrong, it was removed. Training data were then supplemented with additional training data to obtain 50 training points per habitat. These training points were created by selecting pixels on the orthomosaic from easily identifiable habitats and recording location and the associated color composites. To minimize subjectivity and potential misclassification, we re-evaluated the additional training data using kernel density estimates of the GoPro collected training data, where pixels were labeled according to the habitat with the highest kernel density estimate. Only pixels where the visual classification and kernel density estimate agreed were used to supplement the GoPro training data for the supervised image classification. Because macroalgae was sparse in North Harbour and Swift Current in fall, fewer training data could be created (min $n_{macroalgae} = 26$). We then assigned a 10 cm buffer to the training data to cover roughly the same area as the GoPro images and to account for pixel variability within each habitat type.

Finally, we used kernel density curves of the training data to identify the number of classes to include in the model (Fig. 2; see Fig. S2 for kernel density curves). If a curve was bi-modal, we divided the habitat into two separate classes (e.g., exposed eelgrass and submerged eelgrass) to optimize the model classification process (Lillesand and Kiefer 2000). We applied 80% of the training data to build the image classification models and the other 20% for model validation. We then refined our models using a majority filter, which classified pixels while accounting for the class and mode of the adjacent pixels. Each model was evaluated using a confusion matrix, user accuracy, and Cohen's Kappa accuracy (i.e., model accuracy while accounting for the probability that a pixel was classified correctly by chance; Rosenfield and Fitzpatrick-Lins 1986). These metrics were calculated using the "validateMap" function in RStoolbox. Habitats that were divided into two classes according to the bi-modal kernel density curves were then merged back as one habitat (e.g., "submerged" and "exposed" eelgrass became "eelgrass"). We then assessed seasonal changes in eelgrass area coverage between summer and fall by comparing the differences in eelgrass pixels between seasons for each site. Eelgrass area coverage was calculated by multiplying the number of eelgrass pixels by their size (0.01 m^2), and the percent change between seasons was then calculated.

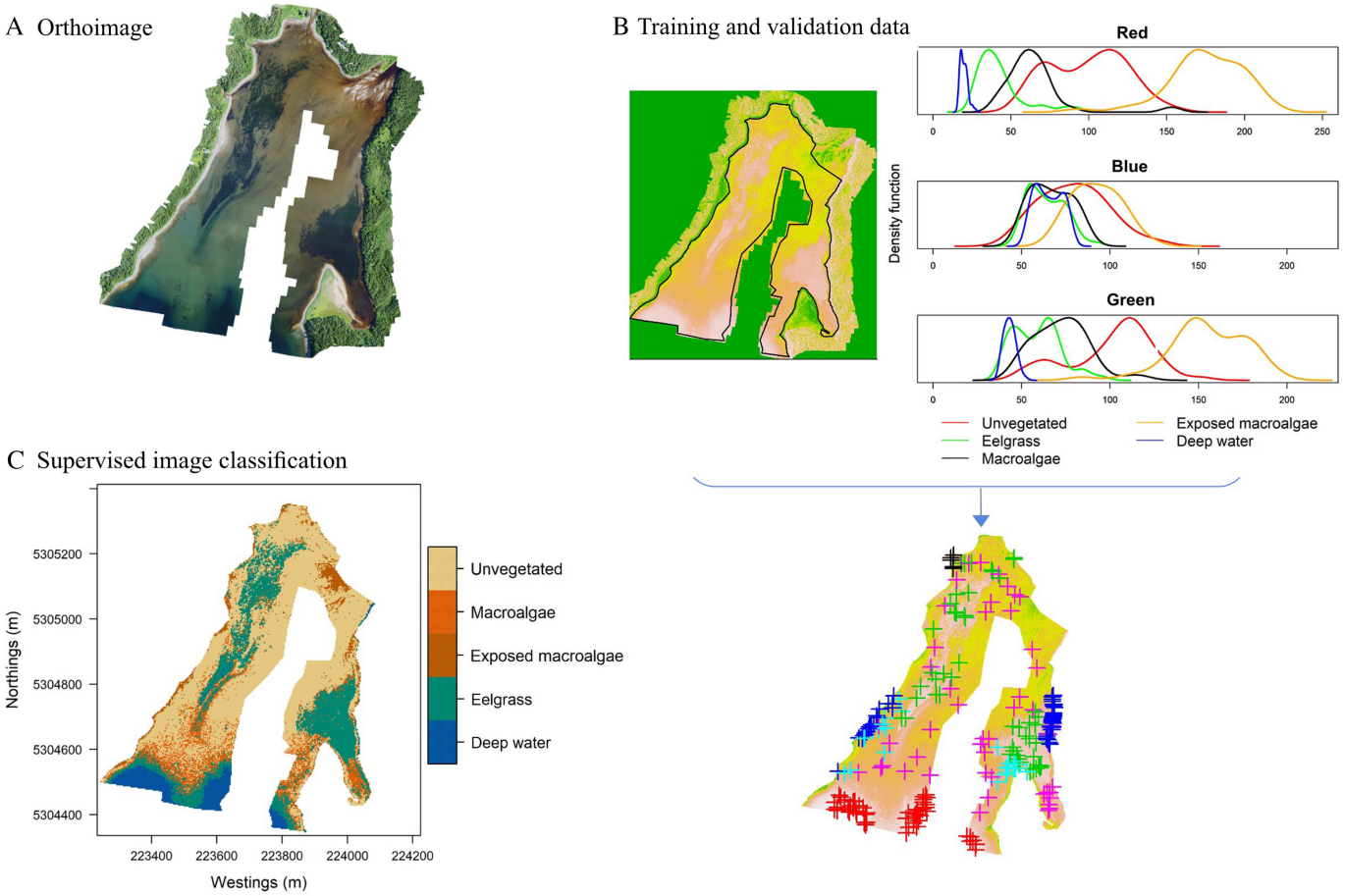

Fig. 2. Workflow for random forest supervised image classification of remotely piloted aircraft system (RPAS) survey imagery. Workflow steps include (A) collecting RPAS imagery and generating the orthoimage, (B) masking land and creating training and validation data, (C) using training data to conduct supervised image classification using random forest analysis to classify the orthoimage and validate the model using validation data.

Comparing RPAS and snorkel transect surveys

We assessed the differences in estimates of benthic habitats between RPAS and the snorkel transect surveys by cropping 1 m^2 quadrats from the classified RPAS model and calculating the percentage of pixels from each habitat class. Quadrat polygons were created in ArcMap mimicking the approach used in the field for the snorkel transect survey. While this approach does not guarantee that locations of the digital quadrats exactly matched those of the snorkel survey, it did allow similar portions of seabed to be compared. We used zero-inflated Poisson (ZIP) regression models to evaluate seasonal changes in eelgrass cover, one per survey method, to relate eelgrass and macroalgae estimates of cover to season, site, and location. These models were used to determine whether both methods indicated similar seasonal changes in eelgrass cover.

Assessing altitude trade-off

Two tests were conducted to evaluate the effects of increasing altitude on benthic classification during RPAS surveys. We conducted these tests at Capelin Cove, a subsite within North Harbour (Fig. 1). The first test compared habitat percent cover from RPAS surveys conducted at four altitudes

(25, 50, 100, and 115 m) with percent cover from snorkel transect surveys – hereafter referred to as the Capelin Cove test. RPAS surveys were conducted sequentially on the same day (Table 1). Camera settings were checked prior to each survey while the RPAS hovered at the survey altitude (e.g., checked at 25 m for the 25 m altitude test; Table S1). To avoid motion blur, flight speeds were decreased at lower altitude (Table 1). There were no GCPs or CPs available for Capelin Cove. We used training data and surveyed two transects (one inside and one edge, $n_{quadrat} = 8$). Otherwise, we used the same procedures for both the RPAS and the snorkel transect surveys previously described, including exporting imagery to 10 cm resolution.

The second test compared classification estimates from RPAS images of a submerged quadrat taken at increasing altitudes – hereafter referred to as the quadrat altitude test. We positioned the submerged quadrat to intersect an eelgrass, macroalgae, and unvegetated boundary (Fig. 3) and collected the RPAS images of the quadrat at ~3 m altitude intervals from 30 to 121 m (Table S1). Camera settings were set while the RPAS hovered at 30 m altitude. We then verified that the same settings also worked for higher altitude images such that all photos were collected using the same camera settings and with the camera pointing nadir. Only autofocus was reset between photos. For each photo, we used a 0.9 m × 0.9 m polygon centered within the quadrat to crop the images such that the quadrat itself (i.e., PVC pipe) would not be included in the image classification. Unlike the Caplin Cove test, image resolution was not altered (Table S1). The cropped images were then classified into the three habitat classes using a random forest unsupervised image classification approach using the "unsuperClass" function in RStoolbox and a majority filter. We calculated the percentage of pixels for each habitat and each altitude and compared these values to the percent cover of each habitat obtained from an underwater image of the submerged quadrat (Fig. 3). Simple linear regression was used to evaluate the relationship between survey altitude and differences in percent cover of each habitat measured using the RPAS versus the underwater image.

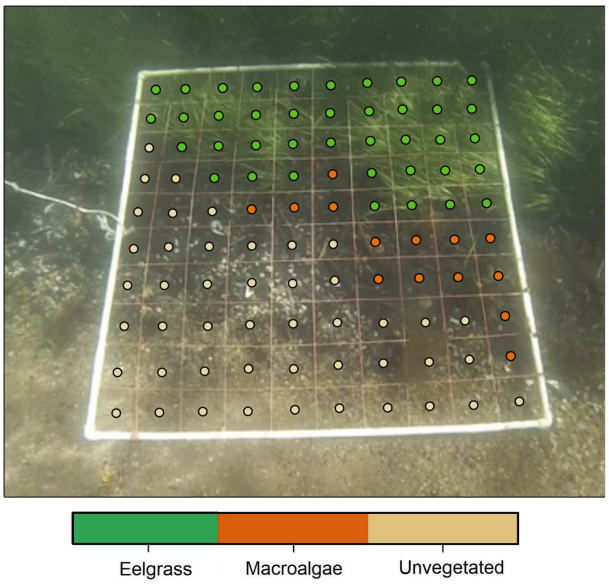

Fig. 3. Image taken from the GoPro video of the 1 m × 1 m submerged quadrat for the quadrat altitude test. Quadrat was divided into a 0.1 m × 0.1 m grid. Colored circles represent the habitat that each square was assigned via visual inspection.

Results

RPAS survey

The RPAS successfully surveyed macro-scale eelgrass meadows while flying at 115 m altitude (Fig. 1). According to the RPAS models, eelgrass extent in North Harbour decreased by 2.6% (−0.30 ha) between the summer and fall, Swift Current increased by 17% (2.1 ha), and Baie de l'Eau decreased by 23% (−5.5 ha) (Table 1).

Spectral separability varied among habitats and sites (Figs. 1, S2), making eelgrass detection more challenging in some sites than others. Spectral separability was highest in North Harbour for summer and fall orthomosaics, which produced the most similar seasonal datasets among the sites. Baie de l'Eau had different levels of spectral separability between eelgrass and unvegetated cover between seasons, and Swift Current orthomosaics showed little separability between habitats in both seasons in areas where the eelgrass was submerged. These differences in spectral separability between sites were reflected in the supervised classification model accuracy, where the overall accuracy and the Cohen's Kappa accuracy were highest for North Harbour (Fig. 4A, B), followed by Baie de l'Eau (Fig. 4C, D) and Swift Current (Fig. 4E, F) surveys, even though they were conducted under similar environmental conditions and low turbidity (Table 2, see Supporting Information for methods of measuring turbidity). Eelgrass misclassification was inconsistent for all models and was highest for Swift Current (Table 3). Inconsistent misclassification negatively affected the reproducibility of the RPAS surveys, resulting in accuracies differing by >10% between seasonal surveys for Swift Current and Baie de l'Eau (Fig. 4). Additionally, inconsistent misclassification rendered it infeasible to distinguish between model confusion versus where, if any, micro/meso-scale changes in seagrass extent or cover occurred (Fig. S3).

In general, the RPAS survey models and the snorkel transect surveys yielded similar percent cover estimates. North Harbour RPAS estimates were most comparable to the snorkel estimates, followed by Baie de l'Eau, and then Swift Current (Fig. S4). Overall, the median absolute value difference in eelgrass percent cover between RPAS and snorkel quadrat estimates indicated that the RPAS yielded a ≥70% classification accuracy for most sites and locations (i.e., edge, middle, outside), with the exception of the inside transect for the Swift Current summer survey (~45%). Macroalgae estimates differed the least between the two methods, with a median RPAS accuracy ≥75% for all cases. Overall, location in the meadow did not have a clear effect on the differences in estimates between the two methods. Despite these similarities, the two methods yielded different seasonal trends in eelgrass and macroalgae percent cover (Fig. 5). However, these differences were not apparent in the ZIP models, which suggested similar conclusions for both survey methods. Specifically, the RPAS estimates of eelgrass cover exhibited a limited effect of season (summer estimate 0.07% higher than fall) and no seasonal effect was detected by the snorkel method (Table 4). A similar trend was observed for macroalgae estimates (0.52%; Table S2). Both methods suggested similar variability in estimates of cover, where more variability in eelgrass cover occurred in the edge transects compared to inside (Fig. 5).

Altitude trade-off

For the Caplin Cove test, photos collected at 25 m altitude did not align to generate an orthomosaic, likely due to low variability in texture and colors among images (Fig. S5A). Comparison between the other RPAS surveys and the snorkel transect survey estimates of habitat cover did not reveal a trend between habitat classification and increasing RPAS survey altitude for transects inside meadows (Fig. 6). However, for edge transects, differences between RPAS and snorkel transect survey estimates of habitat cover decreased with increasing altitude for eelgrass and macroalgae. Inside transects were most similar between the two methods when the RPAS survey was conducted at 100 m altitude and most different when conducted at 115 m, but overall median values were similar (<5% difference).

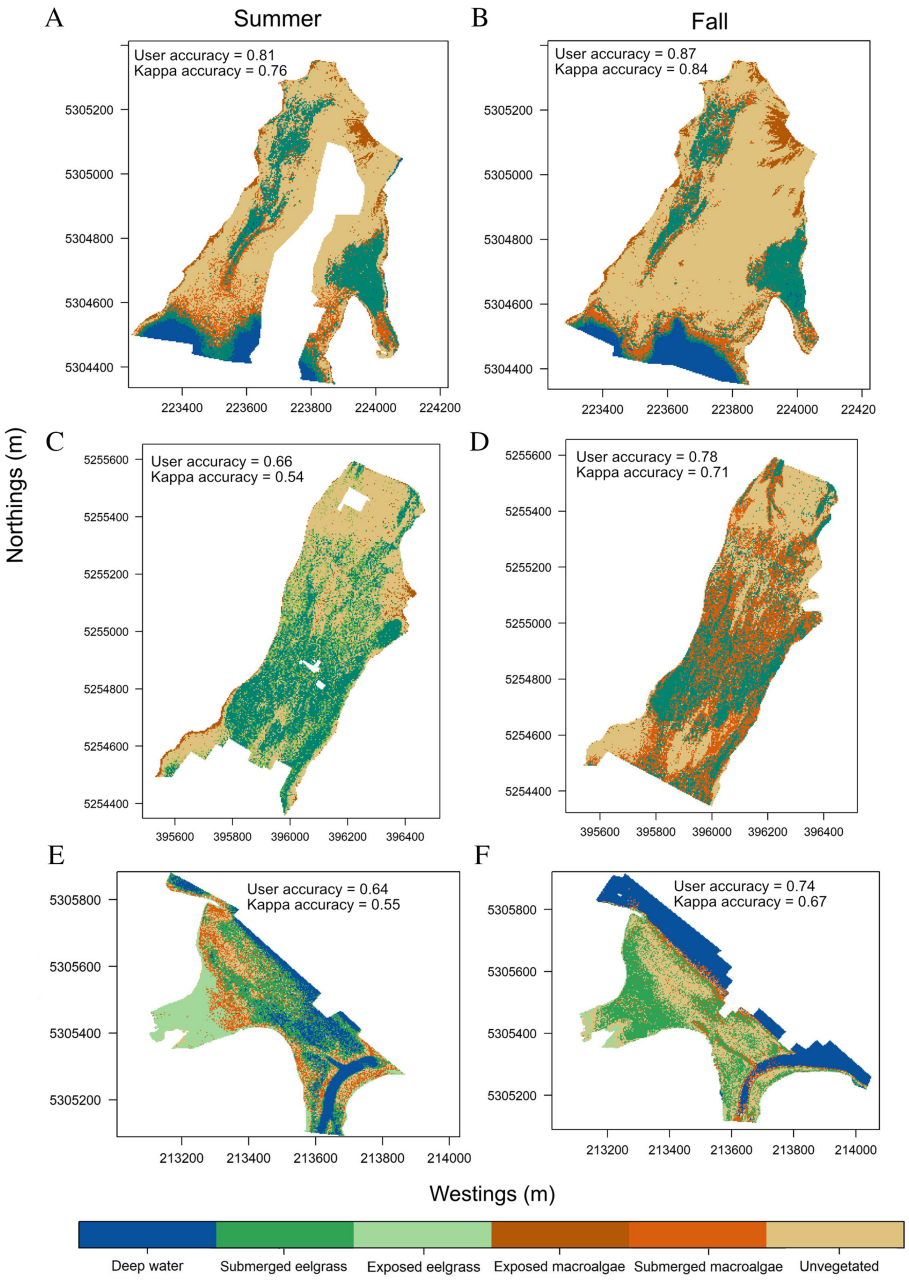

Fig. 4. Random forest supervised image classification of North Harbour (A and B), Bay de l'Eau (C and D), and Swift Current (E and F). Surveys were conducted at 115 m altitude in the summer and the fall.

Therefore, in this first test, higher altitude surveys appeared to improve the accuracy of coverage estimates for the edges of eelgrass meadows and did not affect estimates inside the meadows.

For the quadrat altitude test, there was a positive correlation between altitude and differences in eelgrass cover estimated via the underwater image and RPAS images (Fig. 7). Differences in eelgrass cover estimates increased by 0.09% m^{-1} altitude, increasing from a 19% difference at 30 m to 27%

Table 2. Median water nephelometric turbidity units (NTU) during each remotely piloted aircraft systems (RPAS) survey.

Season	Site	NTU	Stdev
Summer	North Harbour	No data	No data
	Swift Current	0.54	0.12
	Baie de l'Eau	0.21	0.16
Fall	North Harbour	0.14	0.063
	Swift Current	1.03	1.2
	Baie de l'Eau	0.077	0.024

Note: Data were measured using a moored ECO-NTU turbidity sensor (Sea-Bird Scientific, Washington, USA) deployed in each site (Fig. S1). Sensors were programed to record three NTU measurements at 15 min intervals from Swift Current and Baie de l'Eau during June–November 2020 and from North Harbour, during August–November 2020.

Table 3. Confusion matrices for the validation data of the supervised image classification of each site (Figure 3A–F). Orthomosaics were created using a remotely piloted aircraft system (RPAS).

North Harbour Summer					
Prediction	**Deep water**	**Submerged eelgrass**	**Exposed macroalgae**	**Submerged macroalgae**	**Unvegetated**
Deep water	32	1	0	0	0
Submerged eelgrass	0	18	0	4	0
Exposed macroalgae	0	0	30	0	0
Submerged macroalgae	0	1	0	9	11
Unvegetated	0	8	1	0	23
North Harbour Fall					
Prediction	**Deep water**	**Submerged eelgrass**	**Exposed macroalgae**	**Submerged macroalgae**	**Unvegetated**
Deep water	31	0	0	3	0
Submerged eelgrass	0	26	0	1	1
Exposed macroalgae	0	0	29	0	2
Submerged macroalgae	0	6	0	12	2
Unvegetated	0	0	1	2	25
Swift Current Summer					
Prediction	**Deep water**	**Submerged eelgrass**	**Exposed eelgrass**	**Submerged macroalgae**	**Substrate**
Deep water	22	5	0	0	0
Submerged eelgrass	4	16	0	0	5
Exposed eelgrass	0	0	20	2	0
Macroalgae	0	3	10	18	11
Unvegetated	0	4	0	9	18

Swift Current Fall					
Prediction	**Deep water**	**Submerged eelgrass**	**Exposed macroalgae**	**Submerged macroalgae**	**Unvegetated**
Deep water	20	0	0	0	0
Submerged eelgrass	0	18	3	1	6
Exposed macroalgae	0	0	26	0	0
Submerged macroalgae	7	0	0	14	2
Unvegetated	0	13	1	2	22

Baie de l'Eau Summer				
Prediction	**Submerged eelgrass**	**Exposed macroalgae**	**Submerged macroalgae**	**Unvegetated**
Submerged eelgrass	25	0	12	4
Exposed macroalgae	0	24	0	2
Submerged macroalgae	8	0	16	6
Unvegetated	0	6	3	14

Baie de l'Eau Fall					
Prediction	**Submerged eelgrass**	**Exposed macroalgae**	**Submerged macroalgae**	**Substrate**	**Sparse eelgrass**
Submerged eelgrass	13	0	8	0	2
Exposed macroalgae	0	9	0	0	0
Submerged macroalgae	2	0	23	0	5
Unvegetated	0	0	0	3	3
Sparse eelgrass	0	0	1	28	2

at 121 m (Fig. 7). Meanwhile, estimates of macroalgae improved with increasing altitude. Macroalgae estimates were ~10% higher than the underwater imagery at lower altitudes, decreasing by 1.0% m^{-1} altitude. Estimates of unvegetated cover decreased by 0.04% m^{-1} altitude; however, these differences were not statistically significant.

Discussion

This study assessed the feasibility of conducting reproducible RPAS surveys to monitor the seasonal dynamics of eelgrass and adjacent benthic habitats at the meadow-scale (e.g., 50 ha) in a cold, temperate, estuarine ecosystem. Our results demonstrate that the capacity of RPAS to detect seasonal variation in habitat percent cover is highly variable within and among sites. The two survey methods (i.e., RPAS and snorkel transects) used in this study detected a <1% seasonal change in eelgrass percent cover, suggesting negligible variation in seagrass cover and therefore, potentially negligible change in the provision of ecosystem services by eelgrass in Newfoundland between mid-summer and early-fall. Eelgrass in Atlantic Canada reaches peak growth in August before declining in the winter due to sea ice and storms (Murphy et al. 2021). Therefore, our study shows that annual monitoring of eelgrass during peak season could be extended until late September/early October. However, RPAS image classification was challenged by fragmented, heterospecific, and deeper benthic habitats. Inconsistent misclassification rendered locating micro/meso-scale changes infeasible, potentially preventing us from identifying sections of the meadow where seasonal changes in extent and percent cover may have occurred. This would have implications for the reproducibility of any repeated monitoring using RPAS, whether it be seasonal or annual.

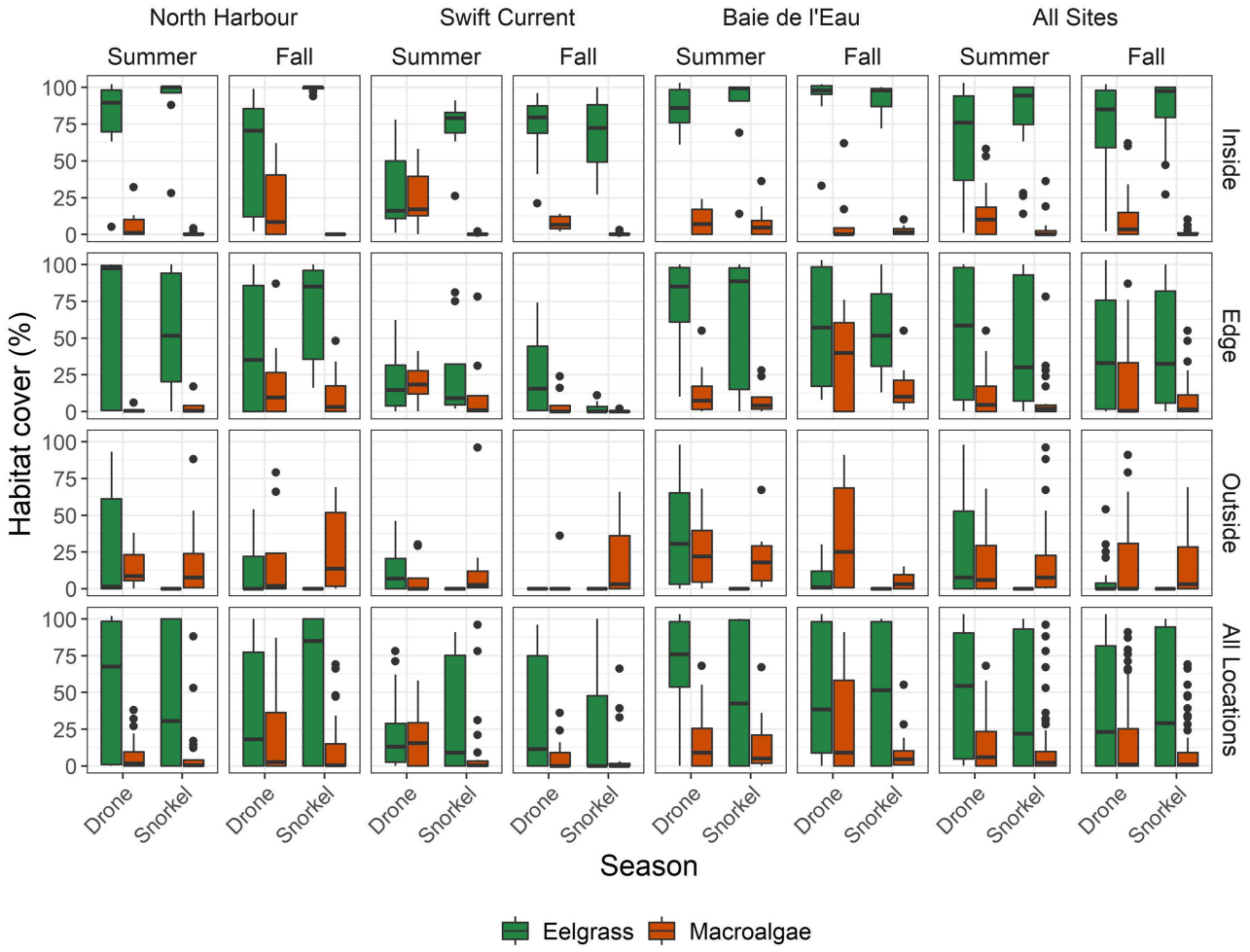

Fig. 5. Boxplots comparing the percent habitat cover (%) of eelgrass (green) and macroalgae (orange) measured each season using a remotely piloted aircraft system (RPAS) at 115 m altitude versus the snorkel quadrat survey. Panels are broken down by survey site, season, and location of the quadrats relative to the eelgrass meadow.

Our results also showed that the effects of flight altitude on accuracy are not straightforward. Macro-scale (i.e., snorkel transect comparison) estimates of cover improved with increased altitude, whereas micro/meso-scale (i.e., submerged quadrat comparison) cover estimates varied depending on the habitat. Flying at higher altitude advantageously reduces survey time to the detriment of image resolution. However, given that accuracy was not necessarily reduced at higher altitude, we suggest that, when monitoring macro-scale changes in benthic estuarine habitats where the environmental conditions are frequently shifting within minutes/hours, the benefit of increased likelihood of successful survey (e.g., image stitching) outweighs the cost of collecting lower resolution imagery. This finding is applicable to any group seeking to use RPAS to monitor macro-scale changes in submerged, estuarine habitats.

Reproducibility

The reproducibility of RPAS surveys is likely limited by a combination of environmental factors. Successfully mapping eelgrass meadows using RPAS has been linked to weather and light

Table 4. Count model coefficients for zero-inflated poisson (ZIP) regression models relating eelgrass percent cover estimates to season, site, and location.

RPAS				
Covariate	**Estimate (%)**	**St. Error (%)**	***P*-value**	***95% CI***
Intercept	4.2	0.028	**<0.001**	[4.15, 4.26]
Summer	0.066	0.025	**0.009**	[0.016, 0.15]
North Harbour	−0.073	0.029	**0.01**	[−0.13, −0.017]
Swift Current	−0.59	0.034	**<0.001**	[−0.65, −0.52]
Inside	0.17	0.027	**<0.001**	[0.12, 0.23]
Outside	−0.60	0.042	**<0.001**	[−0.68, −0.52]
Snorkel				
Covariate	**Estimate (%)**	**St. Error (%)**	***P*-value**	***95% CI***
Intercept	4.05	0.029	**<0.001**	[3.99, 4.11]
Summer	0.0047	0.025	0.85	[−0.045, 0.055]
North Harbour	0.073	0.029	0.011	[0.016, 0.013]
Swift Current	−0.46	0.034	**<0.001**	[−0.53, −0.39]
Inside	0.48	0.027	**<0.001**	[0.43, 0.53]

Note: Two models were conducted for each survey method, remotely piloted aircraft system (RPAS) and snorkel transect survey. Models were generated using a log link. Outside transect data were omitted for the snorkel model because all values of eelgrass were zero.

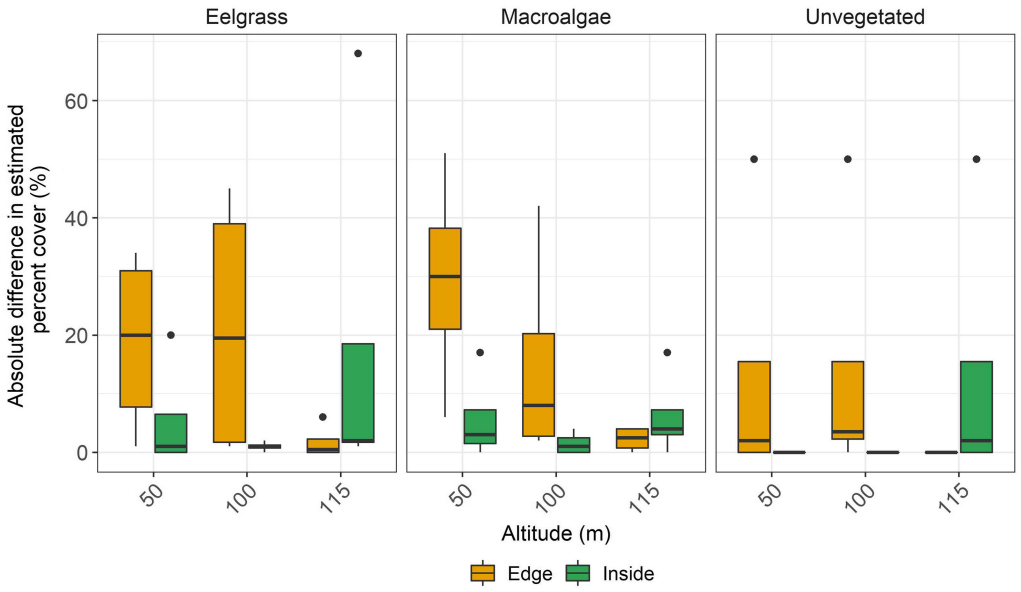

Fig. 6. Relationship of increasing the remotely piloted aircraft system (RPAS) altitude on estimates of eelgrass, macroalgae, and unvegetated percent cover compared to snorkel transect estimates. Boxplots show the percent differences (absoulte values) in estimates between the two survey methods with increasing RPAS survey altitude, where $n_{quadrat/transect} = 4$. Black line represents the median, boxes represent the upper and lower quartiles, whiskers describe the range of the data, and black dots represent outliers. Yellow boxes show differences for transects at the edge of the meadows and green boxes show differences for transects inside the meadows.

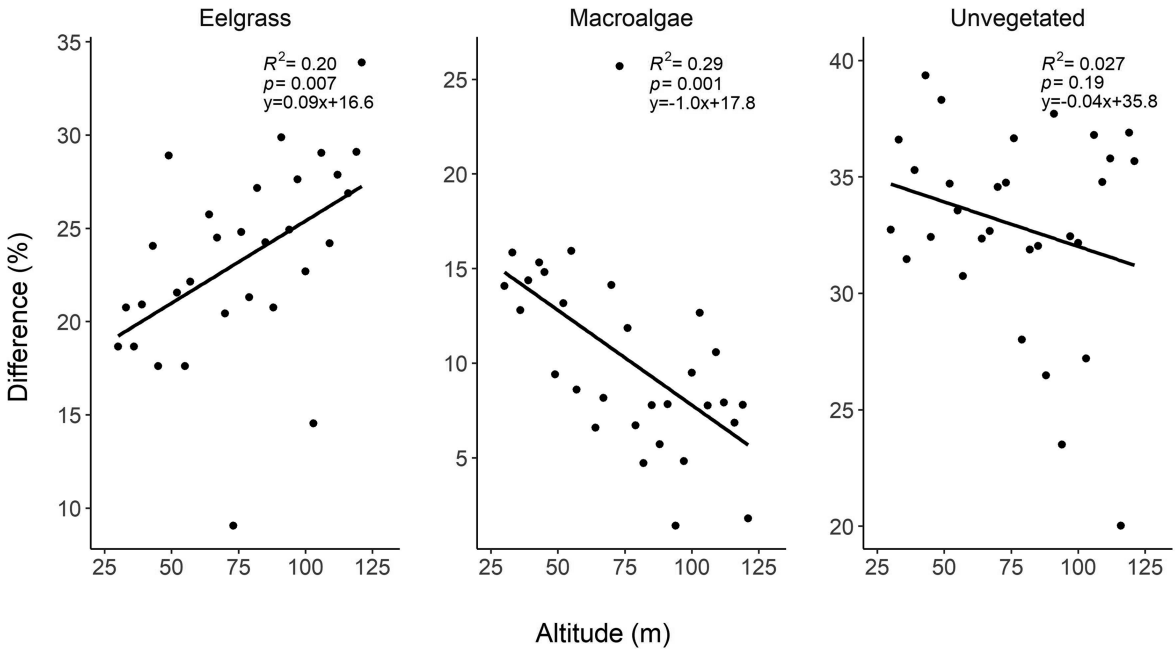

Fig. 7. Relationship between increasing the remotely piloted aircraft system (RPAS) altitude and the absolute value differences in estimates of eelgrass, macroalgae, and unvegetated cover. Differences (%) on the y-axis were calculated as the absolute value of the difference between the habitat cover (%) measured using an RPAS and the percent habitat cover calculated from a GoPro underwater image of the same quadrat (Fig. 3). Black dots represent estimates using RPAS images.

penetrability (Joyce et al. 2018; Nahirnick et al. 2019a, 2019b). Although all surveys in our study were conducted in optimal weather conditions and all our sites were less than 5 m deep, depth was not consistent among surveys as we could not control for tide. Light penetration is reduced with increasing depth, such as high tide or deeper portions of a meadow. This is particularly the case for red wavelengths, which become absorbed or scattered, making deeper sites harder to survey (Duntley 1963; Tait et al. 2019). In shallow portion of the meadow, low tide causes seagrass blades to bend, which increases the likelihood of overestimating seagrass percent cover and extent. As a result, there is no universal ideal tidal height to survey seagrass using RPAS. The effect of tide on seagrass imagery varies depending on the meadow blade length and how much depth varies throughout the meadow. We did not have the data resolution to detect whether water tidal height caused the variability we observed; however, neither did we observe any patterns in our results.

Turbidity, a common feature in coastal temperate regions due to freshwater influx and seasonal phytoplankton blooms, also inhibits light penetrability and is a common feature in coastal temperate regions (Babin et al. 2003; Duntley 1963). Turbidity was low for all surveys (**Table 2**) and therefore was unlikely to have driven the differences in accuracy. However, we did observe seasonal differences in the surface water color, especially in the Baie de l'Eau fall survey (**Fig. 1C**). This was likely caused by influx of tannin-rich freshwater, as observed by the red/brown color of the orthomosaic (**Fig. 1C**), and potentially by the tidal amplitude difference between surveys (1.4 m compared to 0.2 m for the other two sites). Seasonal variation in freshwater influx and mixing generates unique interactions among light, depth, and color. These interactions may have contributed to the seasonal variability in survey accuracy observed in our study.

As observed in other studies, spectral separability between habitats affected image classification (Lillesand and Kiefer 2000; O'Neill and Costa 2013; Tait et al. 2019; Ventura et al. 2018). This in turn affected the reproducibility of our RPAS eelgrass surveys. Spectral signatures showed instances of substantial spectral overlap between habitats, causing classification confusion. Spectral separability between eelgrass and unvegetated cover diminished at the transition from shallow to deep water, creating an erroneous eelgrass boundary between unvegetated habitat and deep water in both of our North Harbour models. However, this was not detected in the confusion matrix, which showed eelgrass classification errors stemming from unvegetated seabed and macroalgae. Therefore, we suggest that model accuracy estimates may be misleading and enforce the importance of refining/validating RPAS surveys with complimentary ground-level surveys. Furthermore, consistent with previous studies (e.g., Barrell and Grant 2015; Duffy et al. 2018; Nahirnick et al. 2019b), sparse habitats or edges were more difficult to differentiate than continuous habitat. This may be because habitats underwater are more likely to appear different in aerial imagery due to light refraction (Ellis et al. 2020; Joyce et al. 2018). Additionally, classification errors are more likely to occur at habitat boundaries, where spectral signatures of boundary pixels are composed of a mixture of habitat types (Woodcock and Strahler 1987), which generates pixels with intermediate tones, confusing the classification model. Thus, our results suggest that reproducible RPAS surveys of either deep (>5 m), fragmented, or more heterospecific eelgrass meadows are more difficult to acquire and seasonal estimates of change may be more prone to error. Separating submerged aquatic vegetation into eelgrass and macroalgae classes likely explains the lower model classification accuracies in our study. Using multispectral sensors may facilitate the detection of submerged benthic habitats in estuarine environments (James et al. 2020; Su et al. 2006), but this is beyond the scope of our study.

Various post-processing workflows have been applied in the literature to classify remote sensing imagery (e.g., Murfitt et al. 2017; Duffy et al. 2018; Ventura et al. 2018; Wilson et al. 2019; Schroeder et al. 2019). Most approaches include some form of manual classification to delineate features of interest or to create training data *post-hoc* based on the analyst's interpretation of the system and imagery (e.g., Konar and Iken 2018; Ventura et al. 2018; Gonçalves et al. 2019; Nahirnick et al. 2019b). This introduces observer bias into the classification process, impacting the reproducibility of the survey. We present a method using kernel density plots to supplement training and validation data *post-hoc*, which minimizes analyst-induced bias. However, some subjectivity was still required to select training data, such as ensuring these data do not come from pixels falling on habitat boundaries (Lillesand and Kiefer 2000), and avoiding clustering training data to avoid overfitting sections of the model. Our study only tested the reproducibility of RPAS surveys using RGB imagery without supplemental information. Supplementing training data with additional habitat-defining characteristics such as depth and optical texture or collecting multispectral imagery to separate habitats (e.g., Tait et al. 2019) would likely improve the reproducibility of RPAS surveys for monitoring submerged eelgrass meadows and adjacent estuarine habitat and may be required when reproducibility is low.

Do results improve with altitude?

Terrestrial and coastal RPAS surveys have shown that lower altitude surveys enable more habitats to be distinguished in the imagery (Duffy et al. 2018; Perroy et al. 2017). However, we found that reducing survey altitude did not always improve agreement in estimates submerged eelgrass and macroalgae percent cover between RPAS surveys and snorkel quadrat surveys. Full site surveys showed that the accuracy of RPAS estimates improved with altitude for the edge transects, while it was unaffected for the inside transects. This could be because finer details such as ripples and shadows on the surface were detected by lower altitude images, increasing spectral variability (Mount 2005; Woodcock and Strahler 1987) and potentially reducing accuracy. For continuous eelgrass meadows, such disturbances are likely minimal on inside transects at lower altitudes given that the pixels are from the same

habitat type. In contrast, the edge of the eelgrass meadow is more fragmented. Therefore, intermediate spectral tones from multiple habitats in a pixel and water disturbance will more likely distort habitat boundaries, altering apparent eelgrass coverage. At a higher altitude, noise from texture features such as ripples would have been reduced as lower resolution images smooth finer details and reduce spectral variability (Woodcock and Strahler 1987). Therefore, the accuracy of RPAS surveys of meadow edges or of fragmented meadows may be improved in higher altitude surveys.

In contrast, the quadrat altitude test suggested that the effect of increasing altitude varied among habitats. Similar results were reported by Ellis et al. (2020) while flying a fixed wing RPAS at similar altitudes as our study. Reduced image resolution with higher altitude increases the number of pixels that encompass a mixture of habitat types, and thus the number of pixels with intermediate color tones, which subsequently reduces classification accuracy (Woodcock and Strahler 1987). We could therefore expect that, in heterogenous meadows, higher altitude would decrease classification accuracy. While this was the case for eelgrass and macroalgae, classification of unvegetated habitat was less affected by changes in image resolution with changing altitude. This is likely because eelgrass and macroalgae have similar spectral signatures regardless of resolution, while unvegetated habitat was more spectrally separable from the other two habitat classes. Nevertheless, in all cases the effect of increasing altitude only changed the estimates of cover by up to 10%. Flying at higher altitudes helps survey larger scale meadows within limited battery life of the RPAS and reduces the risk of environmental conditions that change within minutes (e.g., sun angle, tide, cloud cover) from changing during the survey (Joyce et al. 2018). Therefore, in the case of large, submerged eelgrass meadows, the benefit of surveying at a higher altitude may outweigh the cost of collecting lower resolution imagery, especially given that images collected at lower altitudes can be more challenging to stitch into an orthomosaic.

Conclusions

Seasonal monitoring of seagrass meadow extent and adjacent estuarine habitats is important for coastal habitat management. In Newfoundland, seasonal changes in seagrass extent and cover would be more likely to be detected with survey periods starting earlier in the spring (e.g., April/May) after ice-melt and when eelgrass cover is low, then in the late summer/early fall (e.g., August/September). Issues of ice formation in the late fall/winter when eelgrass die-off (i.e., December) and increased riverine discharge due to snow melt in the spring, in addition to other varying environmental conditions (e.g., tide, wind, cloud), render seasonal monitoring using RPAS extremely challenging in north temperate environments. For these reasons, monitoring using RPAS in this region is optimal in summer/early fall months (i.e., July-early October), when eelgrass is the least fragmented (i.e., peak growth) and environmental conditions are more conducive to RPAS surveys. Similar logic could be applied to other temperate regions as well.

Regardless of the monitoring period, recognizing the limitations of RPAS surveys is crucial for reliable monitoring. We show that sources of variability on RPAS surveys limit reproducibility and therefore limit how much RPAS can be relied on to detect fine-scale changes during management decision-making, including changes in percent cover of seagrass and adjacent benthic habitats. In our study, trends in seasonal changes in seagrass and macroalgae percent cover often differed between RPAS and snorkel transect surveys. Differences in tidal height may have contributed to the variability observed; however, this is a significant challenge and potentially a limitation if RPAS are to be used to monitor submerged coastal habitats in temperate regions, where low wind and no cloud conditions are rare. Supplementing imagery with texture data such as bathymetry maps, Secchi depth, or multispectral imagery could help correct for depth and potentially help overcome reproducibility challenges but come at an additional cost and may be unfeasible for many monitoring groups. Overall, selecting whether to use RPAS surveys to monitor seagrass over time is question dependent.

RPAS appear to be reliable for large-scale surveys to detect macro-habitat characteristics, such as general extent and identifying meadow structure and delineating vegetated versus unvegetated habitat in general. For example, edges and fragmented areas should be monitored via snorkel while large, submerged seagrass meadows can be monitored using higher altitude RPAS imagery. In this case, increasing survey altitude helps mitigate the risk of environmental conditions shifting mid-survey, thereby offsetting the cost of obtaining lower resolution imagery. Meanwhile, RPAS equipped with RGB sensors alone cannot distinguish between macroalgae and seagrass reliably, and estimates of fine-scale habitat changes, such as changes in species composition or eelgrass growth through time, should be interpreted with caution.

Acknowledgements

This project was funded by Fisheries and Oceans Canada as part of Coastal Restoration Fund within the Canadian Ocean Protection Plan and by the National Science and Engineering Research Council of Canada Alexander Graham Bell Canada Graduate Scholarships-Doctoral Program scholarship to T.S.P. We thank Trevor Witt and David Burchfiled (Kansas State University Polytechnic) for drone training, and Dr. Rachel Sipler (Memorial University), Kristen Wilson (Dalhousie University), and Matthew Robertson (Marine Institute of Memorial University) for scientific guidance. We also thank Lucas Vaters, Taylor Hughes, Machaela McDonald, Elanor Dillabough, and Matthew Robertson for field assistance.

Author contributions

A.L., T.S.P., B.F., and R.S.G. conceived the ideas and designed the methodology. T.S.P. and G.A. collected the data. T.S.P. analyzed the data and led the writing of the manuscript. All authors contributed critically to the drafts and gave final approval for publication of the manuscript.

Data accessibility

Data and code have been made publicly available on GitHub (github.com/Tprystay/RPAS_reproducibility).

Conflict of interest

All authors declare no conflict of interest.

Supplementary material

The following Supplementary Material is available with the article through the journal website at doi:10.1139/facets-2022-0149.

Supplementary Material 1

References

Babin M, Morel A, Fournier-Sicre V, Fell F, and Stramski D. 2003. Light scattering properties of marine particles in coastal and open ocean waters as related to the particle mass concentration. Limnology and Oceanography, 48: 843–859. DOI: 10.4319/lo.2003.48.2.0843

Barbier EB, Hacker SD, Kennedy C, Koch EW, Stier AC, and Stillman BR. 2011. The value of estuarine and coastal ecosystem services. Ecological Monographs, 81, 169–193. DOI: 10.1890/10-1510.1

Barrell, J., and Grant, J., 2015. High-resolution, low-altitude aerial photography in physical geography: A case study characterizing eelgrass (*Zostera marina)* and blue mussel (*Mytilus edulis*) landscape mosaic structure. Physical Geography, 39: 440–459. DOI: 10.1177/0309133315578943

Björk M, Short FT, Mcleod E, and Beer S. 2008. Managing seagrasses for resilience to climate change [online]: Available from scholars.unh.edu/cgi/viewcontent.cgi?article=1474&context=jel

Chand S, and Bollard B. 2022. Detecting the spatial variability of seagrass meadows and their consequences on associated macrofauna benthic activity using novel drone technology. Remote Sensing, 14: 160. DOI: 10.3390/rs14010160

Cho HJ, Biber PD, Darnell KM, and Dunton KH. 2017. Seasonal and annual dynamics in seagrass beds of the rand Bay National Estuarine Research Reserve, Mississippi Source: Southeastern Geographer, Vol. 57, No. 3, Special Issue: Coastal Seagrass and Submerged Aquatic Vegetation Habitats in the Gulf. Univ. North Carolina Press 57, 246–272. [online]: Available from aquila.usm.edu/fac_pubs/17217

Colefax AP, Butcher PA, and Kelaher BP. 2018. The potential for unmanned aerial vehicles (UAVs) to conduct marine fauna surveys in place of manned aircraft. ICES Journal of Marine Science, 75: 1–8. DOI: 10.1093/icesjms/fsx100

Duffy JP, Pratt L, Anderson K, Land PE, and Shutler JD. 2018. Spatial assessment of intertidal seagrass meadows using optical imaging systems and a lightweight drone. Estuarine, Coastal and Shelf Science, 200: 169–180. DOI: 10.1016/j.ecss.2017.11.001

Duntley SQ. 1963. Light in the Sea. Journal of the Optical Society of America. 53: 214–233. DOI: 10.1364/josa.53.000214

Ellis SL, Taylor ML, Schiele M, and Letessier TB. 2020. Influence of altitude on tropical marine habitat classification using imagery from fixed-wing, water-landing UAVs. Remote Sensing in Ecology and Conservation, 7: 50–63. DOI: 10.1002/rse2.160

Fourqurean JW, Willsie A, Rose CD, and Rutten LM. 2001. Spatial and temporal pattern in seagrass community composition and productivity in south Florida. Marine Biology, 138: 341–354. DOI: 10.1007/s002270000448

Gonçalves J, Pôças I., Marcos B., Mücher CA., and Honrado JP. 2019. SegOptim - A new R package for optimizing object-based image analyses of high-spatial resolution remotely-sensed data. Int. Appl. Earth Obs. Geoinformation, 76: 218–230. DOI: 10.1016/j.jag.2018.11.011

Hemminga MA, and Duarte CM. 2000. Taxonomy and distribution, in: Seagrass Ecology. Cambridge University Press, New York, pp. 1–20.

James D, Collin A, Houet T, Mury A, Gloria H, and Le Poulain N. 2020. Towards better mapping of seagrass meadows using UAV multispectral and topographic data. Journal of Coastal Research, 95: 1117–1121. DOI: 10.2112/si95-217.1

Joyce KE, Duce S, Leahy SM, Leon J, and Maier SW. 2018. Principles and practice of acquiring drone-based image data in marine environments. Marine and Freshwater Research, 70: 952–963. DOI: 10.1071/mf17380

Kirkman H. 1996. Baseline and monitoring methods for seagrass meadows. Journal of Environmental Management, 47: 191–201. DOI: 10.1006/jema.1996.0045

Konar B, and Iken K. 2018. The use of unmanned aerial vehicle imagery in intertidal monitoring. D Deep Sea Research Part II: Topical Studies in Oceanography, 147: 79–86. DOI: 10.1016/j.dsr2.2017.04.010

Krause JR, Hinojosa-Corona A, Gray AB, and Watson EB. 2021. Emerging sensor platforms allow for seagrass extent mapping in a turbid estuary and from the meadow to ecosystem scale. Remote Sensing, 13: 1–15. DOI: 10.3390/rs13183681

Leutner B, Horning N, and Schwalb-Willmann J. 2022. RStoolbox: Tools for Remote Sensing Data Analysis. R package [online]: Available from CRAN.R-project.org/package=RStoolbox

Li WT, Kim YK, Park JI, Zhang X, Du GY, and Lee KS. 2014. Comparison of seasonal growth responses of *Zostera marina* transplants to determine the optimal transplant season for habitat restoration. Ecological Engineering, 71: 56–65. DOI: 10.1016/j.ecoleng.2014.07.020

Lillesand T, and Kiefer R. 2000. Digital image processing, *In*: Remote Sensing and Image Interpretation. pp. 470–605.

Lyons MB, Roelfsema CM, and Phinn SR. 2013. Towards understanding temporal and spatial dynamics of seagrass landscapes using time-series remote sensing. Estuarine, Coastal and Shelf Science, 120: 42–53. DOI: 10.1016/j.ecss.2013.01.015

Mount R. 2005. Acquisition of through-water aerial survey images: Surface effects and the prediction of sun glitter and subsurface illumination. Photogrammetric Engineering and Remote Sensing, 71: 1407–1415. DOI: 10.14358/pers.71.12.1407

Murfitt SL, Allan BM, Bellgrove A, Rattray A, Young MA, and Ierodiaconou D. 2017. Applications of unmanned aerial vehicles in intertidal reef monitoring. Scientific Reports, 7: 10259. DOI: 10.1038/s41598-017-10818-9

Murphy GEP, Dunic JC, Adamczyk EM, Bittick SJ, Côté IM, Cristiani J, et al. 2021. From coast to coast to coast: ecology and management of seagrass ecosystems across Canada. Facets 6: 139–179. DOI: 10.1139/facets-2020-0020

Nahirnick NK, Hunter P, Costa M, Schroeder S, and Sharma T. 2019a. Benefits and challenges of UAS imagery for eelgrass (*Zostera marina*) mapping in small estuaries of the Canadian West Coast. Journal of Coastal Research, 35: 673–683. DOI: 10.2112/jcoastres-d-18-00079.1

Nahirnick NK, Reshitnyk L, Campbell M, Hessing-Lewis M, Costa M, Yakimishyn J, et al. 2019b. Mapping with confidence; delineating seagrass habitats using Unoccupied Aerial Systems (UAS). Remote Sensing in Ecology and Conservation, 5: 121–135. DOI: 10.1002/rse2.98

Natural Earth. 2021. Natural Earth [online]: Available from naturalearthdata.com/

Nordlund LM, Jackson EL, Nakaoka M, Samper-Villarreal J, Beca-Carretero P, and Creed JC. 2018. Seagrass ecosystem services – What's next? Marine Pollution Bulletin, 134: 145–151. DOI: 10.1016/j.marpolbul.2017.09.014

Nordlund LM, Koch EW, Barbier EB, and Creed JC. 2016. Seagrass ecosystem services and their variability across genera and geographical regions. PLoS ONE, 11: 1–23. DOI: 10.1371/journal.pone.0163091

O'Neill JD, and Costa M. 2013. Mapping eelgrass (*Zostera marina*) in the Gulf Islands National Park Reserve of Canada using high spatial resolution satellite and airborne imagery. Remote Sensing of Environment, 133: 152–167. DOI: 10.1016/j.rse.2013.02.010

Orth RJ, Carruthers TJB, Dennison WC, Duarte CM, Fourqurean JW, Heck KL, et al. 2006. A global crisis for seagrass ecosystems. Bioscience, 56: 987–996. DOI: 10.1641/0006-3568(2006)56[987:agcfse]2.0.co;2

Orth RJ, Lefcheck JS, McGlathery KS, Aoki L, Luckenbach MW, Moore KA, et al. 2020. Restoration of seagrass habitat leads to rapid recovery of coastal ecosystem services. Science Advances, 6: 1–10. DOI: 10.1126/sciadv.abc6434

Perroy RL, Sullivan T, and Stephenson N. 2017. Assessing the impacts of canopy openness and flight parameters on detecting a sub-canopy tropical invasive plant using a small unmanned aerial system. ISPRS Journal of Photogrammetry and Remote Sensing, 125: 174–183. DOI: 10.1016/j.isprsjprs.2017.01.018

Reise K, and Kohlu, J. 2008. Seagrass recovery in the Northern Wadden Sea? Helgoland Marine Research, 62: 77–84. DOI: 10.1007/s10152-007-0088-1

Rosenfield GH, and Fitzpatrick-Lins K. 1986. A coefficient of agreement as a measure of thematic classification accuracy. Photogrammetric Engineering and Remote Sensing, 52: 223–227.

Salinas C, Duarte CM, Lavery PS, Masque P, Arias-Ortiz A, Leon JX, et al. 2020. Seagrass losses since mid-20th century fuelled CO_2 emissions from soil carbon stocks. Global Change Biology, 26: 4772–4784. DOI: 10.1111/gcb.15204

Schroeder SB, Dupont D, Boyer L, Juanes F, Costa M. 2019. Passive remote sensing technology for mapping bull kelp (Nereocystis luetkeana): A review of techniques and regional case study. Glob. Ecol. Conserv. 19: e00683. DOI: 10.1016/j.gecco.2019.e00683

Seifert E, Seifert S, Vogt H, Drew D, van Aardt J, Kunneke A, et al. 2019. Influence of drone altitude, image overlap, and optical sensor resolution on multi-view reconstruction of forest images. Remote Sensing, 11. DOI: 10.3390/rs11101252

Short FT, Koch EW, Creed JC, Magalhães KM, Fernandez E, and Gaeckle JL. 2006. SeagrassNet monitoring across the Americas: Case studies of seagrass decline. Marine Ecology, 27: 277–289. DOI: 10.1111/j.1439-0485.2006.00095.x

Short FT, Coles RG, and Pergent-Martini C. 2001. Global seagrass distribution. Global Seagrass Research Methods. Elsevier.

Sonoki S, Shao H, Morita Y, Minami K, Shoji J, Hori M, et al. 2016. Using acoustics to determine eelgrass bed distribution and to assess the seasonal variation of ecosystem service. PLoS ONE, 11: 1–15. DOI: 10.1371/journal.pone.0150890

Su H, Karna D, Fraim E, Fitzgerald M, Dominguez R, Myers JS, et al. 2006. Evaluation of eelgrass beds mapping using a high-resolution airborne multispectral scanner. Photogrammetric Engineering and Remote Sensing, 72: 789–797. DOI: 10.14358/pers.72.7.789

Tait L, Bind J, Charan-Dixon H, Hawes I, Pirker J, and Schiel D. 2019. Unmanned aerial vehicles (UAVs) for monitoring macroalgal biodiversity: Comparison of RGB and multispectral imaging sensors for biodiversity assessments. Remote Sensing, 11: 2332. DOI: 10.3390/rs11192332

Tan YM, Dalby O, Kendrick GA, Statton J, Sinclair EA, Fraser MW, et al. 2020. Seagrass restoration is possible: Insights and lessons from Australia and New Zealand. Frontiers in Marine Science, 7. DOI: 10.3389/fmars.2020.00617

Tennekes M. 2018. tmap: Thematic Maps in R. Journal of Statistical Software, 84(6): 1–39. DOI: 10.18637/jss.v084.i06

Ventura D, Bonifazi A, Gravina MF, Belluscio A, and Ardizzone G. 2018. Mapping and classification of ecologically sensitive marine habitats using unmanned aerial vehicle (UAV) imagery and Object-Based Image Analysis (OBIA). Remote Sensing, 10: 1331. DOI: 10.3390/rs10091331

Waycott M, Duarte CM, Carruthers TJB, Orth RJ, Dennison WC, Olyarnik S, et al. 2009. Accelerating loss of seagrasses across the globe threatens coastal ecosystems. Proceedings of the national academy of sciences, 106: 12377–12381. DOI: 10.1073/pnas.0905620106

Wilson KL, Skinner MA, and Lotze HK. 2019. Eelgrass (*Zostera marina*) and benthic habitat mapping in Atlantic Canada using high-resolution SPOT 6/7 satellite imagery. Estuarine, Coastal and Shelf Science, 226: 106292. DOI: 10.1016/j.ecss.2019.106292

Woodcock CE, and Strahler AH. 1987. The factor of scale in remote sensing. Remote Sensing of Environment, 21: 311–332. DOI: 10.1016/0034-4257(87)90015-0

Worm B, Barbier EB, Beaumont N, Duffy JE, Folke C, Halpern BS, et al. 2006. Impacts of biodiversity loss on ocean ecosystem services. Science, 314: 787–790. DOI: 10.1126/science.1132294

Yang B, Hawthorne TL, Hessing-Lewis M, Duffy EJ, Reshitnyk LY, Feinman M, et al. 2020. Developing an introductory UAV/Drone mapping training program for seagrass monitoring and research. Drones, 4: 70. DOI: 10.3390/drones4040070

Zimmerman RC, Reguzzoni JL, and Alberte RS, 1995. Eelgrass (*Zostera marina*) transplants in San Francisco Bay: Role of light availability on metabolism, growth and survival. Aquatic Botany, 51: 67–86. DOI: 10.1016/0304-3770(95)00472-C